ORIGINAL ARTICLE

Removal of lead(II) by *Saccharomyces cerevisiae* AUMC 3875

Manal Tawfeek El-Sayed

Abstract The removal of lead(II) from artificial aqueous solution using live and dead biomass of *Saccharomyces cerevisiae* AUMC 3875 was investigated. The minimum inhibitory concentration (MIC) value of *S. cerevisiae* AUMC 3875 for lead(II) was 600 mg/l. For live and dead biomass, maximum lead(II) uptake capacities were achieved at pH 5.0, initial metal ion concentration 300 mg/l, and biomass dosage 3 g/l. Maximum biosorption capacities were reached after 3 h and 20 min for live and dead cells, respectively. Fourier Transform Infrared spectroscopy (FTIR) results revealed the important role of C=O, OH, NH, protein amide II band, PO_2^-, mannans, sulphur and sulphur-oxygen compounds in lead(II) uptake. Scanning electron microscopy analysis (SEM) showed that the cell surface morphology and surface area/volume ratio changed greatly after lead(II) uptake. Transmission electron microscopy analysis (TEM) confirmed the involvement of both extracellular adsorption and intracellular penetration through the cell wall. X-ray powder diffraction (XRD) analysis revealed the presence of $Pb(SO_4)$, Pb_2OSO_4 by dead biomass and $Pb_3O_2(SO_4)$, Pb_2OSO_4 by live biomass. Energy dispersive X-ray microanalysis (EDAX) confirmed the occurrence of sulphur, oxygen and lead(II) on the cell wall. The removal of lead(II) from storage battery industry wastewater was performed by dead biomass efficiently.

Keywords *Saccharomyces cerevisiae* · Lead(II) · Biosorption · Mechanism

Introduction

Large amount of heavy metals are released into the environment due to the technological activities of humans. The impact of these metals in aquatic systems and their accretion throughout the food chain can cause a serious threat to animals and humans, originating a worldwide environmental problem (Machado et al. 2008). Lead(II) is extremely toxic even at low concentrations, and accumulates mainly in bones, brain, kidney and muscles and may cause many serious disorders like anemia, nervous disorders, sickness and kidney diseases particularly in children (Chua et al. 1999).

Conventional methods for removing lead(II) from wastewater include precipitation, ultra filtration and wall processes such as reverse osmosis (Mohammadi et al. 2005). These methods have significant disadvantages, which include incomplete metal removal, high capital cost when applied to high strength wastes with heavy metal concentrations greater than 100 ppm, and generation of toxic sludge or other waste products that require disposal (Goyal et al. 2003). These disadvantages, together with the need for more economical and effective methods for recovery of metal, have resulted in development of alternative separation technologies. In this respect, biosorption, a biological method of environmental control, has emerged as an alternative to conventional effluent treatment methods, as it has the advantage of low operating cost, is effective in diluted solutions, generates minimum secondary waste, complexes within a short time period, and has no toxicity limit for heavy metals (Volesky 1990). Biosorption is an operation that combines the use of biomaterials for sorbing, sequestering and immobilizing organic or inorganic substances from aqueous solutions. This type of uptake may take place by any one or a combination of different processes, such as complexation, coordination, chelation, ion exchange or microprecipitation and entrapment. All these mechanisms except the last two are associated with either living or dead microbial cells. It is necessary to distinguish between active, metabolically mediated metal uptake by living cells as opposed to passive metal sequestering by dead biomass (Naja and Volesky 2011). Naja and Volesky also added that actively metabolizing cells may, in some instances, even

M. T. El-Sayed (✉)
Botany Department, Faculty of Science, Zagazig University,
Zagazig, Egypt
e-mail: tawfeek.manal1@gmail.com

actively repel metals ions, particularly the more toxic ones, as a self defense. When the cells are inactivated, the chemical binding sites of the biomass may attract metal ions from the solution. Fungal biosorption have been studied extensively because of the availability of large amount of waste fungal biomass from fermentation industries and the amenability of microorganisms to genetic and morphological manipulation. Biosorption potential of fungi like *Rhizopus*, *Aspergillus*, *Streptoverticillum*, *Phanerochaete* and *Saccharomyces* have been explored many times (Pakshirajan and Swaminathan 2010). *Saccharomyces cerevisiae* has found to be the efficient biosorber of heavy metals like Au, Mn, Cu, Co, Pb (Parvathi et al. 2006; 2007; Ezzouhri et al. 2008; Mishra et al. 2009).

In light of this, the present study has been carried out to investigate the potential of live and dead *Saccharomyces cerevisiae* AUMC 3875 for removal of lead(II) from aqueous solution and storage battery industry wastewater. Experimental parameters affecting the biosorption process, such as pH, biosorbent dose, initial metal concentration and contact time, were studied. The biosorption mechanism was also investigated by using scanning electron microscopy (SEM), transmission electron microscopy (TEM), fourier transform infrared spectroscopy (FTIR), X-ray powder diffraction (XRD) and energy dispersive X-ray microanalysis (EDAX).

Materials and methods

Chemicals

Stock metal solutions of lead(II) were prepared by dissolving appropriate quantities of lead(II) nitrate salt in double distilled water. The stock solutions were diluted further with deionized distilled water to obtain working solutions of different concentrations.

Development of biosorbent

Saccharomyces cerevisiae AUMC 3875 was obtained from Assuit University Mycological Centre. For mass culturing, *S. cerevisiae* AUMC 3875 was cultivated in liquid medium using the shake flask method. *S. cerevisiae* AUMC 3875 was grown in an incubator shaker at 30 °C and 150 rpm. The liquid medium used for growth contained 6.0 g yeast extract, 15.0 g sucrose, 0.52 g $MgSO_4 \cdot 7H_2O$, 3.0 g K_2HPO_4, 3.76 g NaH_2PO_4, 3.35 g $(NH_4)_2SO_4$ and 0.017 g $CaCl_2 \cdot 4H_2O$ per liter of distilled water. The pH of the medium was adjusted to 5.0 with aqueous solution of 0.1 N H_2SO_4 and NaOH. After growth period of 24 h, *S. cerevisiae* AUMC 3875 cells were separated from liquid medium by centrifugation at 5,000 rpm for 10 min, and

washed twice with distilled water. One part was autoclaved to prepare dead cells and other part was directly used as live cells. Cell viability was assessed by conventional spread plate technique using distilled deionized water as a diluent (Suh et al. 1998).

Experimental methods

Determination of minimum inhibitory concentration (MIC)

A sterilized solution of lead(II) nitrate was aseptically added to the sterilized medium to get the final concentration of 0, 200, 400, 500, 600, 700, 800, 900, 1,000 and 1,100 μg/ml. The plates were inoculated with 100 μl of yeast suspension and incubated at 30 °C for 48 h. Minimum inhibitory concentration (MIC) was identified as the minimum concentration of lead(II) that inhibited visible growth of *S. cerevisiae* AUMC 3875.

Batch biosorption procedure

All uptake experiments were performed by suspending the biosorbent in 100 ml of metal solution at desirable pH, biosorbent dose, initial metal ion concentration and contact time. Sorption contact experiments with metal bearing solutions were run in triplicate and the mean values were considered. Standard error bars are indicated (Ezzouhri et al. 2008; Padmavathy et al. 2003)

Optimization of pH

In order to evaluate the effect of pH on metal uptake, the pH of the solution was adjusted in the range between 3 and 6 viz. 3, 4, 5 and 6 before mixing biomass. The pH was adjusted to the required value with aqueous solution of 0.1 N HNO_3 and 0.1 N NH_4OH. Initial metal ion concentration 300 mg/l and biosorbent dose was 3 g/l at 28 °C and contact time was 20 min in the case of dead cells and 3 h for live cells. The concentration of unadsorbed lead(II) in the supernatants was measured by using an atomic adsorption spectrophotometer (Model Unicam 969, Centric Laboratory of Agriculture Faculty, Zagazig University).

Optimization of biosorbent dose

The prepared microorganism suspension of live and dead biomass (50 ml) with concentrations 2, 3, 4 and 5 g/l (with respect to cell dry weight) were added to 500 ml Erlenmeyer flasks separately. Aliquots (50 ml) of lead(II) nitrate solution prepared at twice the desired concentration (300 mg/l) were added to each flask, and shaken in a rotary shaker incubator at 30 °C and 150 rpm (Suh et al. 1998) for 20 min in the case of dead biomass and 3 h in the case of live biomass.

Optimization of metal ion concentration

The batches were set at different initial metal ion concentrations of lead(II). Aliquots (50 ml) of 50, 150, 250, 300 and 350 mg/l concentrations of lead(II) nitrate were added to 3 g/l biomass at 28 °C in 500 ml Erlenmeyer flasks.

Optimization of contact time

The biomass suspension (3 g/l) was contacted with lead(II) solution (300 mg/l) for different periods of time. Samples were analyzed at different time intervals of 0.17, 0.33, 0.5, 1.0, 1.5, 2.0, 3.0, 6.0, and 12 h and the adsorption profile was monitored. For all graphical representations, the mean values of the three replicates of the batch experiments were plotted.

Biosorption data evaluation

The amount of metallic ions biosorbed per gram of biomass (q) was determined using the following equation:

$$\text{Biosorption capacity(q)} = \frac{C_i - C_f}{M} V$$

Where, C_i is the initial metal ion concentration (mg/l), C_f is the final metal ion concentration (mg/l), M is the mass of the biosorbent (g), V is the volume of the metal solution and q is biosorption capacity (mg/g).

FTIR spectroscopy

Infrared of live and dead native cells, as well as live and treated ones, were recorded over the region 400–4,000 cm^{-1} with Pelkin-Elmer FTIR 1650 spectrophotometer. The samples were examined in KBr discs. Discs containing 3 % (w/w) of finely ground powder of each sample were prepared.

Scanning electron microcsopy (SEM)

Saccharomyces cerevisiae AUMC 3875 cells were fixed in 2.5 % glutaraldehyde at 4 °C for 24 h and then post-fixed in 1.0 % osmium tetraoxide at room temperature for 1 h (Harley and Freguson 1990). The specimens were then dehydrated with ascending concentrations of acetone, and finally sputter-coated with gold. The Scanning and photographing were done using Jeol scanning electron microscope (JEM-1200XII).

Morphometric analysis

To calculate cell volume (v) and surface area (A) by the following equation, normal and stressed yeast cell dimension were measured directly form the SEM photographs:

$$V(\pi m^3) = \pi r^2 h$$

$$A(\pi m^2) = 2\pi r^2 + 2\pi r h$$

Where r and h are radius and length of a cell in μm (Neumann et al. 2005). Mean cell dimension of the S. cerevisiae AUMC 3875 were measured. Average cellular volume and surface area were calculated from normal cells. Cells showing deformations/depression were not considered.

Transmission electron microscopy (TEM)

Saccharomyces cerevisiae AUMC 3875 cells were fixed in 2.5 % glutaraldehyde for 3 h (Gupta and Berridge 1966), washed twice with 0.2 M phosphate buffer of pH7.4 for 30 min, then post-fixed in 1.0 % osmium tetraoxide for 2 h (Palade 1952). After that, the cells were washed with phosphate buffer for 30 min. All the previous steps of fixation were carried out at 4 °C. Samples were dehydrated in a graded ethanol series (50 %, 60 %, 70 %, 80 %, 90 %, 95 % and 100 %). They were passed in three changes of acetone: ethanol (1:2, 1:1 and 2:0) for 10 min each and embedded in epoxy medium (Epon 812) (Luft 1961). Blocks were sectioned with a diamond knife (ultramicrotome RMC USA) into ultrathin section about 70 nm. These ultrathin sections were constructed with uranyl acetate (Sptempack and Ward 1969) followed by lead(II) citrate (Reynolds 1963) each for 30 min. Transmission and photographing were done using JEOL TEM −1400 electron microscope and optronics AMT CCD camera with 1632 pixel format as side mount configuration.

X-ray powder diffraction analysis (XRD)

X-ray diffraction pattern of powder samples of metal-free control and metal-sorbed live and dead biomass were recorded in a Broker D8 Advanced target Cukα powder diffractometer (λ=1.5418 A°) over the range of 0–80(2θ).

Energy dispersive X-ray microanalysis

Metal-loaded live and dead biomass were used for energy dispersive X-ray microanalysis using X-ray micro analyzer (Model Oxford 6587 INCA x-sight) attached to JEOL JSM-5500 LV scanning electron microscope at Regional Center of Mycology and Biotechnology, Cairo, Egypt.

Application of lead(II) removal capacity by dead biomass of S. cerevisiae AUMC 3875

Wastewater was obtained from storage battery factory in Industrial area of Tenth of Ramadan, Sharkia, Egypt.

Physicochemical parameters of wastewater viz temperature, pH, and the concentration of other metal ions present at the wastewater were measured (Table 1). The concentrations of other metal ions present at the tested wastewater were so small that they could not affect the removal of lead(II) from the wastewater.

Results and discussion

Lead(II) tolerance by *S. cerevisiae*

Results showed high fungal tolerance to lead(II) concentration up to 600 mg/l of lead(II), which is 1,000-fold higher than the concentration permitted in the industrial effluents (0.5 mg of lead(II) per liter of effluent). Comparable results were obtained by Wang and Chen (2006). Biological mechanisms implicated in fungal tolerance include extracellular precipitation, complexation and crystallization, the transformation of metal species, biosorption to cell walls, intracellular chelation by the generation of metallothioneins and phytochelatins, and metal localization/sequestration within vacuoles (Gadd 1992; Liu and Culotta 1999). Colonies developed in the presence of high lead(II) concentrations become much darker than control ones. Such dark colour is probably due to the intensification of pigments on cell wall as response to the stress applied by lead(II) (Ezzouhri et al. 2008).

Effect of biosorbent dose

Results on the influence of biomass dose showed that when the amount of biosorbent increased from 2.0 to 3.0 g/l, the uptake capacity of lead(II) by live and dead biomass increased (Fig. 1). This could be due to the availablility of more binding sites for the biosorption to occur (Cruz et al. 2004; Yahya et al. 2009). Also, it can be seen that biosorption capacity decreased from 27 to 18 mg/g and 19 to 12 mg/g for dead and live biomass respectively, as the biomass concentration increased from 3 to 5 g/l (Fig. 1). This decrease might be due an increase in electrostatic interactions between cells at higher concentrations, causing cells to agglomerate, which contributed to a decrease in the amount of binding sites available (Cho et al. 2010). It was reported that higher specific
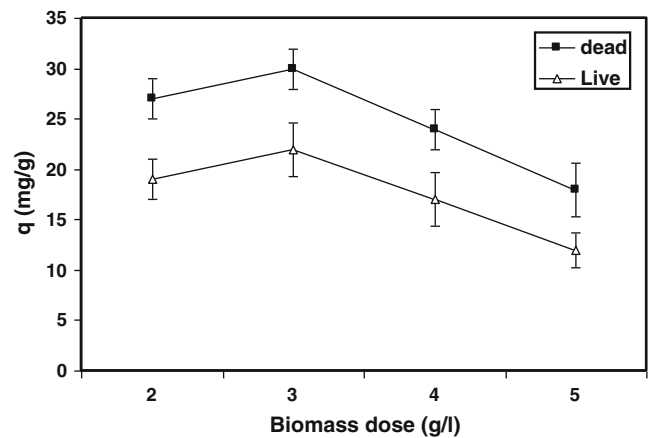

Fig. 1 Effect of biosorbent dose (m) on lead(II) uptake capacity of live and dead biomass of *S. cerevisiae*. Biosorption conditions: initial metal ion concentration (C_i)=300 mg/l; pH=5.0; contact time (t)=20 min (for dead cells) and 3 h (for live cells)

sorption at lower biomass concentrations could be due to an increased metal to biosorbent ratio (Puranik and Paknikar 1999). Mashitah et al. (1999) reported that higher biosorbent dose could produce a "screening" effect on cell wall, protecting the binding sites, thus resulting in lower lead(II) uptake. However, Fourest and Roux (1992) reported that the reduction in metal sorption with increasing biomass concentration is due to an insufficiency of metal ions in solution with respect to available binding sites.

Effect of initial metal ion concentration

Figure 2 indicated that the initial metal ion concentration had a strong effect on the biosorption capacity. As the metal ion concentration increased, biosorption capacity also increased
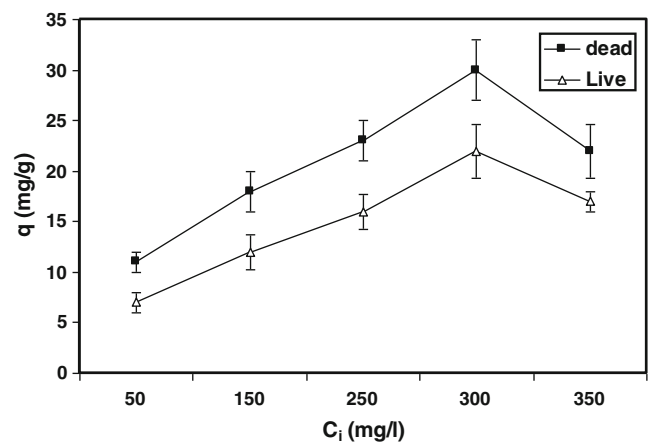
Table 1 Characteristics of used wastewater

Character	Value
Temperature	35 °C
pH	1.7–1.8
Lead(II) (mg/l)	3.77
Chromium	0.011
Cadmium	—

Fig. 2 Effect of initial metal ion concentration (C_i) on lead(II) uptake capacity of live and dead biomass of *S. cerevisiae*. Biosorption conditions: m=3.0 g/l; pH=5.0 and t=20 min (for dead cells) and 3 h (for live cells)
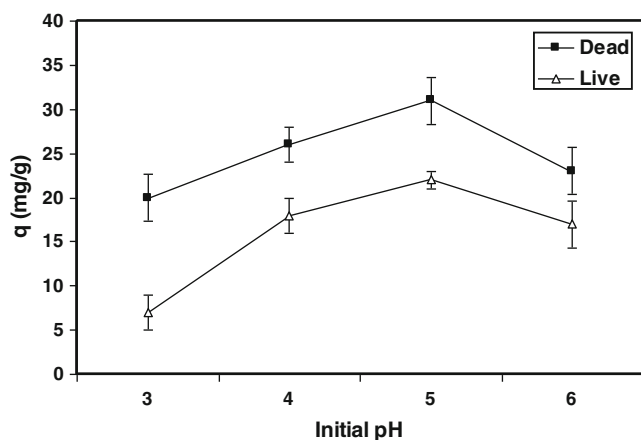
Fig. 3 Effect of initial pH on lead(II) capacity of live and dead biomass of *S. cerevisiae*. Biosorption conditions: C_i=300 mg/l; m= 3 g/l and t=20 min (for dead cells) and 3 h (for live cells)

and reached a saturation value of 30 mg/g and 22 mg/g for dead and live biomass respectively, which were achieved at 300 mg/l concentration of lead(II). The uptake capacity was reduced with the rise in initial metal ion concentration to 350 mg/l. At lower initial solute concentration, the ratio of the initial moles of solute to the available surface area was low; subsequently, the fractional sorption become independent of the initial concentration. At higher concentration, the sites available for sorption become fewer compared to the moles of solute present and, hence, the removal of solute was strongly dependent upon the initial solute concentrations (Binupriya et al. 2007). The reduction in uptake capacity with the rise in initial lead(II) concentration is probably due to rapid saturation of the binding sites of the biosorbent (Ray et al. 2005). Comparable results were reported (Parvathi et al. 2006; Ezzouhri et al. 2008; Dhankhar et al. 2011).

Effect of initial pH

Initial pH value of the solution is an important controlling factor in the biosorption process. The results showed that the adsorptive capacity of dead and living *S. cerevisiae* biomass increased with the rise of pH from 3.0 to 5.0 and decreased at pH 6.0 (Fig. 3). Low pH (3.0) had a more drastic effect on the adsorption capacity of live cells (7.0 mg/g) than on that of dead ones (20 mg/g). This is due to the protein denaturation at low pH (Rothschild and Mancinelli 2001).

Additionally, at low pH, H^+ ions would compete with metal ions, and binding sites are available to metal ions only in deprotonated state (Ofomaja and Ho 2007). With an increase in initial pH, protonation effect becomes minor and the negative charge density on the biomass surfaces increases and more metal binding sites become available (Say et al. 2001). The optimum pH value was 5.0, at which the adsorption capacities were 31 mg/g and 22 mg/g for

dead and live cells, respectively. pH values can affect metal speciation. An increase in pH can result in the precipitation of metal hydroxides. Consequently, less soluble amounts of metals will be available for accumulation in the yeast cells (Sheng et al. 2004).

Effect of contact time

The biosorption capacity of dead and live biomass as a function of contact time is presented in Fig. 4. The primary fast phase of biosorption by dead biomass occured within the first 20 min, and this was followed by second slow phase until equilibrium. A Similar trend was observed by Wang et al. (2010). Equilibrium time was found to be 1 h. On contrary, the rate of biosorption by live biomass was slow and reached the equilibrium within 3 h. Metal ion uptake on yeast is known to involve an initial rapid phase (passive uptake), followed by much slower phase (active uptake). The first stage is physical adsorption or ion exchange at the surface of the biomass and accounted for the major part in total metal uptake, while the second one contributed to a small part (Goyal et al. 2003).

Electron microscopy analysis

SEM analysis was carried out to observe the differences in the surface morphology after the metal uptake by dead and live biomass (Fig. 5). Prior to lead(II) accumulation, *S. cerevisiae* AUMC 3875 had smooth cell surface with no membrane dentitions and uniform electron dense area throughout the unicellular body of the stain (Fig. 5a). Also, the cells were overlapped with each other. After lead(II) uptake, the dead cells became rough due to the aggregates of metal complex deposited in the form of granules (Fig. 5b). This confirmed the important role of *S. cerevisiae* AUMC 3875 cell wall in the
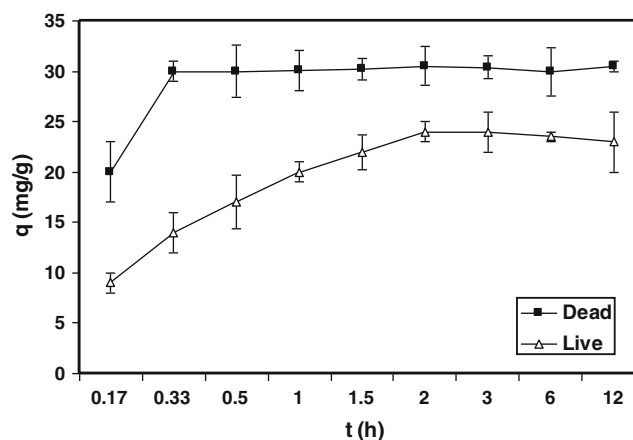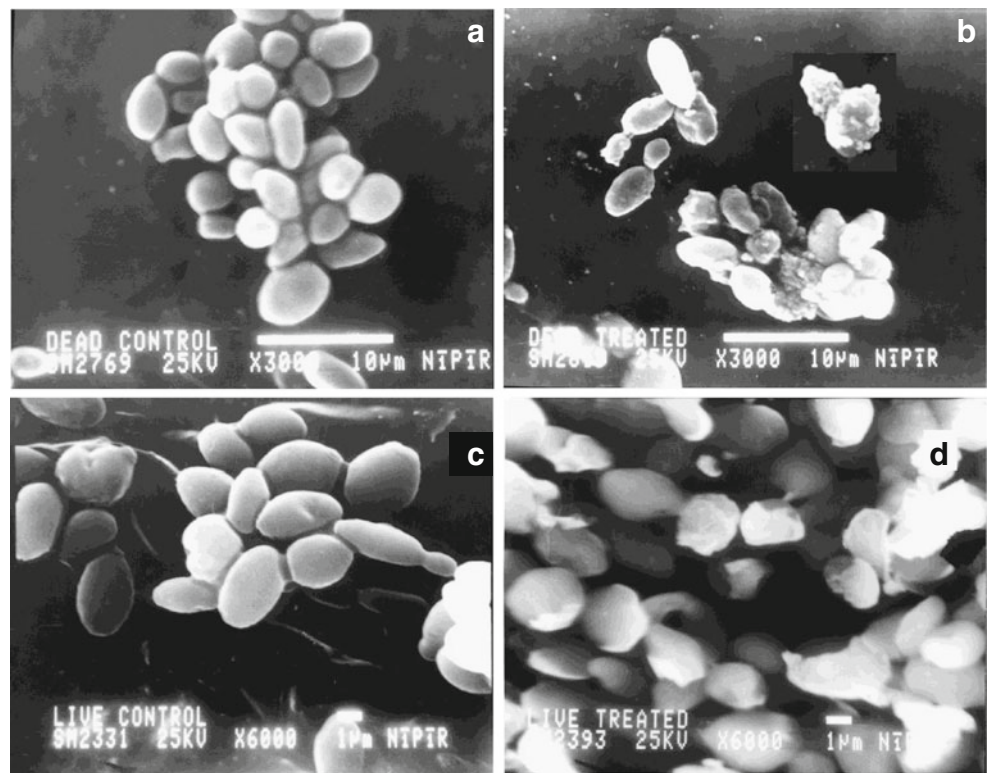

Fig. 4 Effect of contact time (t) on lead(II) capacity of live and dead biomass of *S. cerevisiae*. Biosorption conditions: C_i=300 mg/l; m= 3 g/l and pH=5.0

Fig. 5 SEM of *S. cerevisiae* AUMC 3875 (**a**) native dead cells, (**b**) after lead(II) biosorption, (**c**) native live cells, (**d**) after lead(II) biosorption (25kv)

adsorption process. Similar findings were observed by Limin et al. (2009). Additionally, the dead cells became loosely packed. In live cells, the rupture of cell wall was very evident; consequently, the cells showed wrinkled and rough appearance (Fig. 5d). Also, the cell shape was progressively deformed. The disruption of cellular and organelle membranes

Fig. 6 TEM of *S. cerevisiae* AUMC 3875: (**a**) native dead cells, (**b**) after lead(II) biosorption, (**c**) native live cells, (**d**) after lead(II) biosorption (100kv)
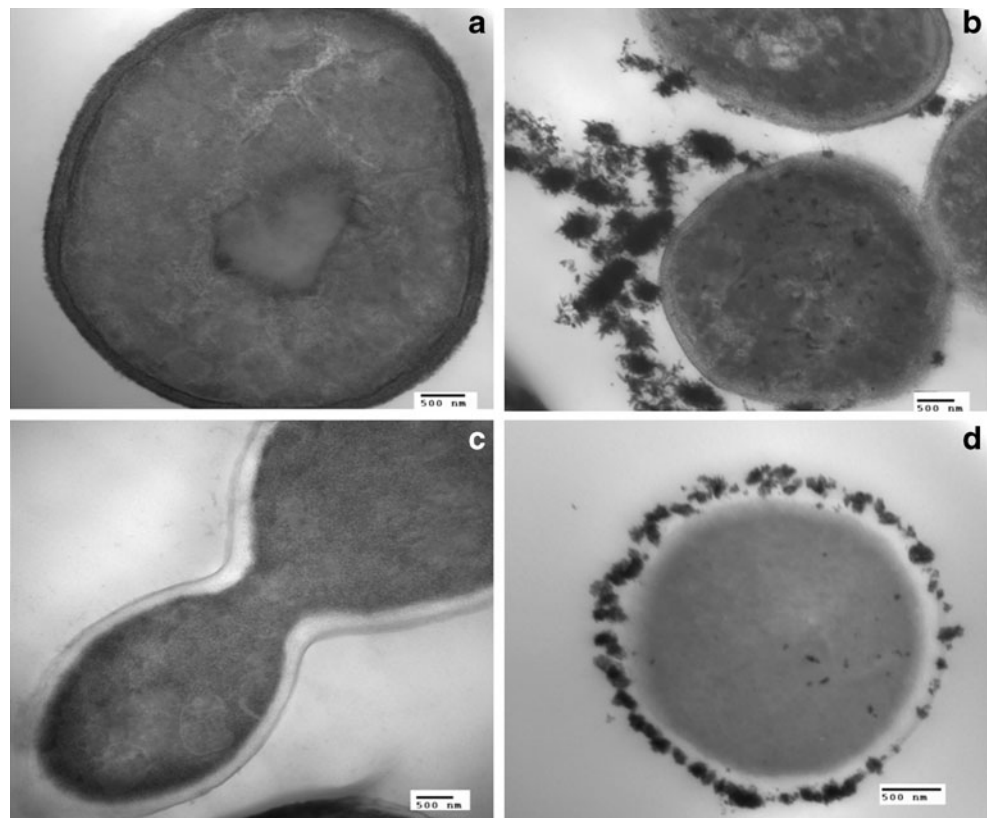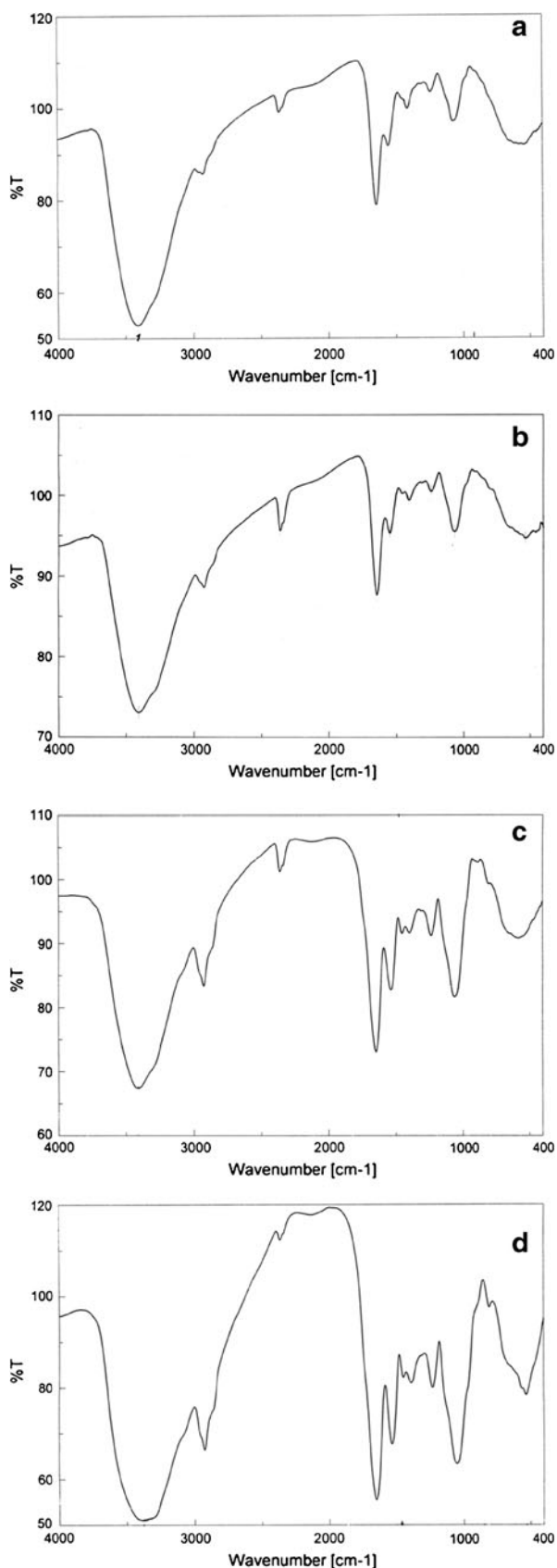
Fig. 7 FTIR spectrum of *S. cerevisiae* biomass (**a**) native live, (**b**) lead (II) loaded live, (**c**) native dead, (**d**) lead(II) loaded dead

are among toxic effects of heavy metals on fungi (Gadd 1992). Similar observations were reported by Suh et al. (1999); Dai et al. (2009); and Lin et al. (2010). Average dimension of normal live cells was 3.8–3.9 μm by 1.2–1.13 μm (Fig. 5) and the surface area/volume ratio was 9.4. In lead(II) stressed cells average dimension was 2.5–2.6 μm by 1.02–1.04 μm the surface area/volume ratio was 8.4. The relative decrease in cell volume plays a key role in the consequent reduction in attachment/uptake sites on the cell surface for the heavy metals and lowering the toxic effects of environmental stress factors (Neumann et al. 2005; Chakravarty and Banerjee 2008).

TEM Observations of original and lead(II) loaded dead and live cells of *S. cerevisiae* AUMC 3875 are represented in Fig. 6. Lead(II) was deposited on the inside and outside of dead (Fig. 6b) and live cells (Fig. 6d) of *S. cerevisiae* AUMC 3875. From TEM micrographs of dead cells, it can be seen that extracellular adsorption of lead(II) occurred mainly in the parts with complete cell walls (Fig. 6d). A variety of ligands located on the cell wall are known to be involved in metal biosorption (Remacle 1990). The presence of lead(II) deposits within the dead cells may be due to the loss of membrane integrity, which leads to the enhancement of metal removal (Machado et al. 2008). Concerning the live cells, Fomina et al. (2005) reported that the fungal biomass can act as a metal sink by metal biosorption to biomass cell walls, intracellular sequestration and accumulation and precipitation of metal compounds onto and/or around hyphae.

FTIR spectroscopy results

As the yeast wall composition was reported by Brady et al. (1994) to contain a large number of complex organic compounds and their polymers, like glucan (28.8 % w/w), mannans (31 %), proteins (13 %), lipids (8.1 %), chitin and chitosan (2 %) and inorganic ions such as Ca^{2+}, Mg^{2+}… etc. (3 %), the FTIR is highly complex. In spite of its high complex nature, the spectra contain information of yeast components that are represented by specific peaks in the fingerprinting regions: region between790 and 1,180 cm^{-1} corresponding to the sugar component of the cells; between 1,200 and 1,290 cm^{-1} corresponding to the nucleic acids; between 1,400 and 1,700 cm^{-1} corresponding to the protein component; between 2,500 and 3,800 cm^{-1} corresponding to −OH and −NH groups and hydrogen bonding; finally peaks at 2,900 cm^{-1} may be because of chitin (Brugnerotto et al. 2001; Galichet et al. 2001; Padmavathy et al. 2003). The peaks at 810, 586 and 537 cm^{-1} may be traced to stretching and bending modes, respectively, of the phosphate moiety (Nakamoto 1963).

The infrared spectra of the control and lead(II)-loaded samples in the case of live and dead biomass are shown in Fig. 7, and their bands assignments are listed in Table 2. The infrared

Table 2 Infrared frequencies (cm^{-1}) and tentative assignments for (A) native dead cells (B) dead treated cells (C) native live cells (D) live treated cells

A	B	Shift	C	D	Shift	Assignment
3415 w	3387 vw1	28	3413 w	3407 w	6	ν (O-H)
2928 vs	2927 vs	1	2928 w	2926 m	2	ν (N-H)
2361 m	2363 w	2	2361 m	2360 s	1	
1647 s	1652 vs	5	1644 v	1641 s	3	ν (C = O) of amide groups
1536 s	1536 s	–	1550 s	1543 s	7	Amide II: N-H and C-N vibrations of the peptide bond in different protein conformations.
1453 s	1451 s	2				Various CH2/CH3 bending vibrations in lipids and proteins.
			1409 s	1402 m	7	C(CH3)2 stretching in proteins.
1396 m	1392 m	4				C = O of COO- symmetric stretching in proteins
1238 s	1235 s	3	1239 m	1239 m	–	PO$_2^{2-}$ in DNA and RNA and phospholipids
1062 m	1052 s	10	1072 m	1062 m	10	β(1 → 3) glucan and S = O
925 w	–	–	–	–	–	ν P = S
–	875 sh					Mannans, phosphorus and ν P = S
–	810 m					
586 br	–		–	–	–	ν (Pb-O) + ring deformation, and ν C-S
	537 m		537 br	535 br	2	

s strong, *w* weak, *sh* shoulder, *v* very, *br* broad, *ν* stretching

spectra of the dead and live biomass are compared with those of the free dead and live biomass in order to determine the sites of donation that may be involved in the interaction. There are some guide peaks in the spectra of the control that are of good help for achieving this goal. The position or the intensities of these peaks are expected to be changed upon of the interaction of biomass with lead(II); also, new peaks are found in the spectra of lead(II)-loaded samples, which gave an indication on chelating between oxygen-containing or nitrogen-containing, sulphur-containing or phosphorous-containing ligands of biomass with metal ions. The marked shift to a lower wave number at 3,415 cm^{-1} for dead cells and at 3,413 cm^{-1} for live cells may be because of the interaction of −NH and −OH groups with lead(II). A small shift of bands at 2,928 cm^{-1} for dead and live cells was indicative of the interaction between –NH group of chitin present in yeast cell wall with lead(II). An increase in the wave number from 1,647 to 1,652 cm^{-1} for dead cells and a slight decrease in the wave number from 1,644 to 1,641 cm^{-1} indicated the involvement of C=0 of amide groups in lead(II) uptake. The decrease in the wave number from 1,550 to 1,543 cm^{-1} in live cells is only owing to the presence of protein amide II band (mainly C-N and N-H vibrations of the peptide bond in different protein conformations). Shifting of band at 1,453 cm^{-1} in dead cells may be because of the involvement of various CH$_2$/CH$_3$ bending vibrations in lipids and proteins in lead(II) biosorption. In live cells, a peak shift to lower wave number (1,409−1,402 cm^{-1}) indicated that C(CH$_3$)$_2$ stretching mainly in proteins could be play a

role in lead(II) biosorption. Still in the protein region, peak shift in dead cells from 1,396 to 1,392 cm^{-1} pointed out that C=O of symmetric stretching in proteins was important in lead(II) biosorption . Only, in dead cells a peak shift from 1,238 to 1,235 cm^{-1} may be because of the involvement of PO$^-_2$ in DNA and RNA and phospholipids in lead(II) biosorption. In live cells and dead cells, large peak shifts to lower wave number were observed in sugar; 1,062 to 1,052 cm^{-1} (dead cells) and 1,072 to 1,062 cm^{-1} (live cells) indicated that both β(1→3) glucan (the major structural component of the cell wall (30–45 % of the wall mass)) and sulphur-oxygen compounds (sulfoxides, S=0) interact with lead(II). The disappearance of band at 925 cm^{-1}, and appearance of a new peak at 810 cm^{-1} were due to P=S stretching . An appearance of new shoulder in FTIR of dead cells at 875 cm^{-1} after lead (II) uptake indicated the intervention of phosphorus and P=S stretching in the process . The disappearance of peak at 586 cm^{-1} and appearance of new peak at 537 cm^{-1} (dead cells) and a small peak shifts 537 to 535 cm^{-1} (live cells) are indicative of C-S stretching, Pb-O and ring deformation in dead cells.

Metal ions adsorb first to the cell surface by interaction with metal-functional groups such as carboxyl, phosphate, hydroxyl, amino, sulphur, sulphide, thiol, etc., and then penetrate the cell membrane and enter into the cells (Wang and Chen 2006). Complexation, ion change adsorption in organic microprecpitation, oxidation and/or reduction have
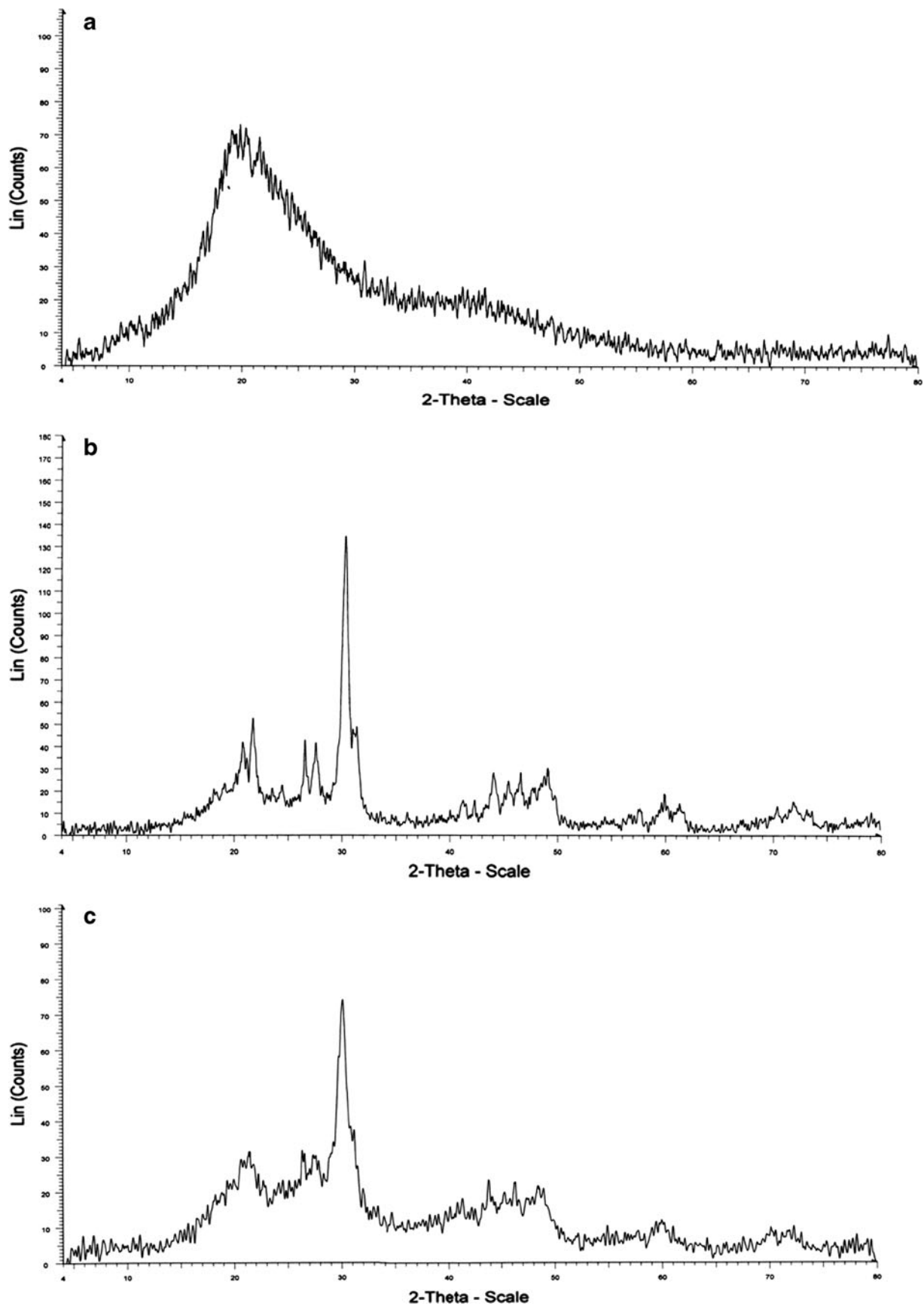
Fig. 8 XRD analysis of *S. cerevisiae* biomass (**a**) native (**b**) lead-loaded live, (**c**) lead-loaded dead
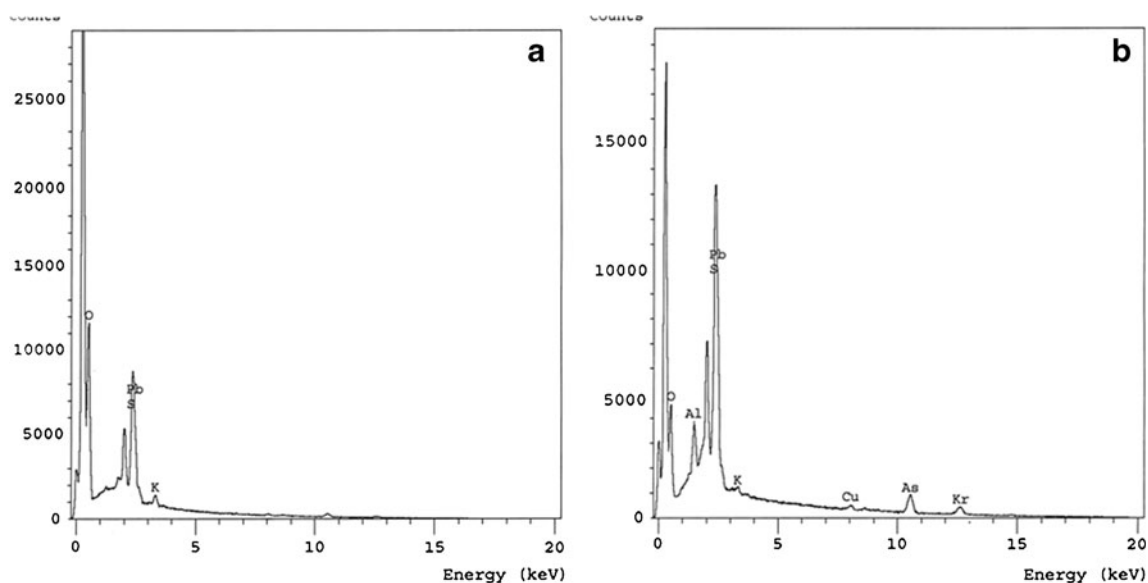
Fig. 9 EDAX analysis of *S. cerevisiae* biomass (**a**) lead-loaded live, (**c**) lead-loaded dead

been proposed to explain the metal uptake process (Liu et al. 2002). FTIR spectra of *S. cerevisiae* revealed that cell walls were the major sorption sites of uranium, and $-O-H$, $C=O$ and PO^{2-} contributed to the major binding groups (Lin et al. 2010). Limin et al. (2009) mentioned that COOH, $C=O$, C-O and N-H are the main active binding sites for the process of lead(II) adsorption by *S. cerevisiae*. The increase of nickel removal by dead cells of *S. cerevisiae* could likely be attributed to the exposition of further metal-binding sites present inside the cells (Machado et al. 2008).

X-ray diffraction (XRD) analysis

To elucidate the chemical nature of yeast cell bound lead, test biomass were subjected to X-ray diffraction analysis before (control) and after lead sequestration (Figs. 8a, b, c and d). In contrast to untreated control biomass, which is expectedly amorphous (Fig. 8a), XRD spectrum for live and dead biomass loaded with lead showed distinct reproducible patterns typical for the presence of crystallized materials. Following lead accumulation, the XRD pattern of live yeast biomass (Fig. 8b) showed eight distinct peaks at 2 θ; 20.70, 21.67, 26.53, 27.54, 30.30, 31.31, 41.19 and 44.08 A° and corresponding to respective d-spacing 4.29, 3.36, 2.95 and 2.19 A°. Based on spacing values, these peaks are attributed to the presence of crystalline lead sulphate compounds ($Pb_3O_2SO_4$ and Pb_2OSO_4) (Characteristic lines at 41.4, 52.1, 42.6, 41.7, 135, 47.8, 15.1 and 27.4 A°). Lead loaded dead biomass (Fig. 8c) showed 5 distinct peaks at 2 θ; 21.40, 26.15, 27.71, 30.09 and 43.82 A°, and corresponding to d-spacing 4.15, 3.40, 3.22, 2.97 and 2.06 A°. Based on spacing values these peaks are attributed to the presence of crystalline lead sulphate compounds; $Pb(SO_4)$ and Pb_2OS_4 (characteristic lines at 29.8, 32,

30.2, 74.1 and 23.1 A°). FTIR spectroscopic analysis of the tested biomass also indicated involvement of cellular sulfur–oxygen compounds in lead binding as described above.

Energy dispersive X-Ray microanalysis (EDAX) was employed to estimate the elemental content of the biomass sample. X-ray peaks showed a broadening in the peak Full Wave Height Maximum (FWHM), which confirmed and was proportional with the size of pellets of the $PbSo_4$ compounds. Also, the height of the peak was proportional with the weight percent of the compound or its ingredients Pb, S and O. Figures 9a and b represented EDAX spectra and concentrations of semi-quantified results of lead-loaded live and dead biomass. This bulk technique gives an elemental ratio of the population as a whole and when analyzing the whole pellet following metal exposure. EDAX spectrum of lead-loaded live biomass (Fig. 9a) showed distinct peaks for: oxygen, sulfur and lead with element % 63.8, 1.48 and 34.72, respectively. Also, EDAX spectra of lead-loaded dead biomass (Fig. 9b) showed distinct peaks for oxygen, sulfur and lead, with element % 30.87, 1.85 and 67.48, respectively. EDAX show an excellent agreement with the corresponding XRD analysis, which confirmed the presence of $Pb_3O_2SO_4$ and $PbOSO_4$ on live biomass and $Pb(SO_4)$ and Pb_2OSO_4 on dead biomass.

References

Binupriya AR, Sathishkumar M, Kavitha D, Swaminathan K, Yun SE, Mun SP (2007) Experimental and isothermal studies on sorption

of Cango red by modified mycelial biomass of wood-rotting fungus. Clean 35:143–150

Brady D, Stoll AD, Starke L, Duncan JR (1994) Chemical and enzymatic extraction of heavy metal binding polymers from isolated cell walls of *Saccharomyces cerevisiae*. Biotechnol Bioeng 44:297–302

Brugnerotto J, Lizardi J, Goycoolea FM, Argulles-Monal W, Desbrieres J, Rinaudo M (2001) An infrared investigation in relation with chitin and chitosan characterization. Polymers 42(8):3569–3580

Chakravarty R, Banerjee PC (2008) Morphological changes in an acidophilic bacterium induced by heavy metals. Extremophiles 12:279–284

Cho DH, Kim EY, Hung YT (2010) Heavy metal removal by microbial biosorbents. In: Wang et al. (eds) Handbook of Environmental Engineering. Springer science + Business Media Vol. 11. pp 375–402

Chua LWH, Lam KH, Bi SP (1999) A comparative investigation on the adsorption of lead (II) by filamentous fungal biomass. Chemosphere 39:2733–2736

Cruz CCV, Da Costa ACA, Henriques CA, Luna AS (2004) Kinetic modeling and equilibrium studies during cadmium biosorption by dead *Sargassum* sp. Biomass. Bioresour Technol 91:249–257

Dai QW, Dong FQ, Zhang W (2009) Biosorption of lead ions on dried waste beer yeast the analysis by FTIR. Spectrosc Spectr Anal 29(7):1788–1792

Dhankhar R, Hooda A, Solanki R, Sainger PA (2011) *Saccharomyces cerevisiae*: a potential biosorbent for biosorption of uranium. Int J Sci Technol 3(6):5397–5407

Ezzouhri L, Castro E, Moya M, Espinola E, Guerrouj M, Rossi B, Lairini K (2008) Uptake of lead by *Saccharomyces cerevisiae* isolated from Tangier Brewery Wastewater. Eur J Sci Res 19(4):668–682

Fomina MA, Alexander IJ, Colpaert JV, Gadd GM (2005) Solubilization of toxic metal mineral and metal tolerance of myocorrhizal fungi. Soil Biol Biochem 37:851–866

Fourest E, Roux JC (1992) Heavy metal biosorption by fungal mycelia by-product: mechanisms and influence of pH. Appl Microbiol Biotechnol 37:399–403

Gadd GH (1992) Metals and microorganisms: a problem of definition. FEMS Microbiol Lett 100:197–204

Galichet A, Sockalingum GD, Belarbi A, Manfait M (2001) FTIR spectroscopic analysis of *saccharomyces cerevisiae* cell walls: study of an anomalous strain exhibiting a pink colored cell phenotype. FEMS Microbiol Lett 197(2):179–186

Goyal N, Jain SC, Banerjee UC (2003) Comparative studies on the microbial adsorption of heavy metals. Adv Environ Res 7:311–319

Gupta BL, Berridge MJ (1966) Fine structural organization of the rectum in the blowfly *Calliphora erythrocephala* (Meig) with special reference to connective tissue, trachea and neurosecretory innervation of the rectal papillae. J Morphol 120(1):23–81

Harley MM, Freguson IK (1990) The role of SEM in pollen morphology and plant systematic. Oxford University Press, Oxford, pp 45–68

Limin D, Juan D, Xin B, Naili Y, Chunhui F, Ying Z (2009) Mechanism of Pb(II) biosorption by *Saccharomyces cerevisiae*. ESIAT" 09 proceeding of the 2009 International Conference on Environ Sci Inf Appl Technol. 01: 712–715

Lin M, Dong F, Yan X, Zeng W, Hou L, Paug X (2010) Biosorption of uranium by *Saccharomyces cerevisiae* and surface interactions under culture conditions. Bioresour Technol 101(22):8573–8580

Liu XF, Culotta VC (1999) Mutational analysis of *Saccharomyces cerevisiae* Sm f1p. a member of the Nramp family of metal transporters. J Mol Biol 289:885–891

Liu R, Tang H, Lao W (2002) Advances in biosorption mechanism and equilibrium modeling for heavy metals on biomaterials. Prog Chem 14(2):87–92

Luft JH (1961) Improvements in epoxy resin embedding methods. J Biophys Biochem Cytol 9:409–414

Machado MD, Janssens S, Soares HMVM, Soares EV (2008) Removal of heavy metals using a brewer's yeast strain of *Saccharomyces cerevisiae*: advantages of using dead biomass. J Appl Microbiol 106(6):1792–1804

Mashitah MD, Zulfadhly Z, Bhatias S (1999) Ability of *Pycnoporus sanguineus* to remove copper ions from aqueous solution. J Artif Cells Blood Substit Immobil Biotechnol 27(5/6):429–433

Mishra A, Pradhan N, Kar RN, Sukla LB, Mishra BK (2009) Microbial recovery of uranium using native fungal strains. Hydrometallurgy 65:175–177

Mohammadi T, Moheb A, Sadrzadeh M, Razmi A (2005) Modeling of metal for removal from wastewater by electrodialysis. Sep Purif Technol 44:73–82

Naja G, Volesky B (2011) The mechanism of metal cation and anion biosorption, In: Kotrba et al. (eds) Microbial Biosorption of Metals. Springer-Verlag, Germany, chap 3:19–58

Nakamoto K (1963) Infrared spectra of inorganic and coordination compounds. John Willey and Sons, New York, pp 103–110

Neumann G, Veeranagonda Y, Karegoudar TB, Sahin Ö, Mausezahl I, Kabelitz N, Kappelmeyer U, Heipieper HJ (2005) Cells of *Pseudomonas putida* and *Enterobacter* sp. adapt to toxic organic compounds by increasing their size. Extremophiles 9:163–168

Ofomaja AE, Ho YS (2007) Effect of pH on cadmium biosorption by coconut copra meal. J Hazard Mater 139:356–362

Padmavathy V, Vasudevan P, Dhingra SC (2003) Biosorption of nickel (II) ions on Baker's yeast. Process Biochem 38(10):1389–1395

Pakshirajan K, Swaminathan T (2010) Biosorption of lead by the immobilized fungus *Phanerochaete chrysosporium* in a packed bed column. Int J Environ Technol Manag 12:214–238

Palade GE (1952) A study of fixation for electron microscopy. J Exp Med 95(3):285–298

Parvathi K, Nagendran R, Nareshkumar R (2006) Lead biosorption onto waste beer yeast by-product, a means to decontaminate effluent generated from battery manufacturing industry. Electron J Biotechnol 10(1):1–14

Parvathi K, Nareshkomar R, Nagendran R (2007) Biosorption of manganese by *A. niger* and *S. cerevisiae*. World J Microbiol Biotechnol 23:671–676

Puranik PR, Paknikar KM (1999) Biosorption of lead, cadmium and zinc by *Citrobacter* strain MCMB-181: Characterization Studies. Biotechnol Prog 15:228–237

Ray L, Paul S, Bera D, Chattopadhyay P (2005) Bioaccumulation of Pb(II) from aqueous solutions by *Bacillus cereus* M$_{16}^{1}$. J Hazard Res Substit 5:1–21

Remacle L (1990) The cell wall and metal binding. In: Volesky B (ed) Biosorption of heavy metals. CRC, Boca Raton, FL, pp 83–92

Reynolds ES (1963) The use of lead citrate at high pH as an electron opaque stain in electron microscopy. J Cell Biol 17:208–212

Rothschild L, Mancinelli RL (2001) Life in extreme environments. Nature 409:1092–1101

Say R, Denizli A, Arica MY (2001) Bio-sorption of cadmium (II), lead (II) and copper (II) with the filamentous fungus *Phanerochaete chrysosporium*. Bioresour Technol 76(1):67–70

Sheng PX, Ting TP, Chen JP, Hong L (2004) Sorption of lead, copper, cadmium, zinc and nickel by marine algal biomass: characterization of biosorptive capacity and investigation of mechanism. J Colloid Interface Sci 275:13–141

Sptempack JG, Ward RT (1969) An improved staining for electron microscopy. J Cell Biol 22:679–701

Suh JH, Kim DS, Yun JW, Song SK (1998) Process of Pb²⁺ accumulation in *Saccharomyces cerevisiae*. Biotechnol Lett 20(2):153–156

Suh JH, Yun JW, Kim DS, Song SK (1999) A comparative study on Pb²⁺ accumulation between *Saccharomyces cerevisiae* and *Aureobasidium pullans* by SEM (Scanning Electron Microscopy) and EDX (Energy dispersive X-ray) analysis. J Biosci Bioeng 87(1):112–115

Volesky B (1990) Biosorption and biosorbents In: Volesky B (ed) Biosorption of heavy metals. Boca Raton: CRC press. pp 3–5

Wang J, Chen C (2006) Biosoprtion of heavy meals by *Saccharomyces cerevisiae:* A review. Biotechnol Adv 24(5):427–451

Wang J, Hu X, Xie S, Bao Z (2010) Biosorption of uranium by immobilized *A. fumigatus* beads. J Environ Radioact 01:504–508.

Yahya MI, Ezeh GC, Musa YF, Mohamed SY (2009) Analysis of heavy metals concentration in road sides soil in Yauri, Nigeria. Afr J Pure Appl Chem 4(3):22–30